THE 3RD INTERNATIONAL CONFERENCE ON MATERIAL HANDLING & INTERNATIONAL CONFERENCE ON FREIGHT PIPELINE

(ICMH/ ICFP'99) Shanghai, China

October. 19-23, 1999

SPONSOR

Chinese Mechanical Engineering Society (CMES)

SUPPORTER

National Natural Science Foundation of China

COSPONSORS

Australian Society for Bulk Solids Handling
Beijing Materials Handling Research Institute
Center for Bulk Solids and Particulate Technologies (Australia)
China Coal Society
Fraunhaufer Institute (Germany)
Hong Kong Institution of Engineers
Institute of Asia Pacific Studies, Wasada University (Japan)
Institution of Electrical Engineers (UK)
Institution of Mechanical Engineers (UK)
International Freight Pipeline Society
Japan Society of Multiphase Flow
Japanese Material Handling Society
Material Handling Institution of CMES
Shanghai Jiaotong University
Society of Manufacturing Engineers (USA)
The Japan Society of Mechanical Engineering

Chairman of ICMH/ICFP'99 Shanghai

LU Yansun Honorary President of CMES

International Program Committee

DING Peifan Deputy General Secretary of CMES
(Chairman)

VISUALIZATION OF WALL SHEAR STRESS USING DISCRETE WAVELETS TRANSFORM

Koichi KATO, Motoaki KIMURA, Masahiro TAKEI, Norimasa MIYAGI and Mitsuaki OCHI
Department of Mechanical Engineering
College of Science and Technology, Nihon University
Kanda Surugadai, Chiyoda-ku, Tokyo 101-8308, Japan

Chih-Ming HO
Mechanical and Aerospace Engineering Department
University of California, Los Angeles
Los Angeles, California 90095, USA

Yoshifuru SAITO
Department of Electrical & Electronic Engineering
Hosei University
Tokyo Japan

Kiyoshi HORII
Shirayuri College
Tokyo Japan

Abstract: Stripe structure in turbulent boundary layer has been clearly visualized by a combination of MEMS(Micro-Electro-Mechanical-Systems) chip and discrete wavelets transform . In detail , the shear stress distribution is decompose with frequency level . The stripe structure at Re=17400 has a small scale in comparison with Re=8700 . The MEMS chip is hardware to measure share stress in boundary layer . But , the measured data are integral values to be ambiguous . The discrete wavelets transform is a technique to make it clear .

Key word: Discrete Wavelets Analysis , Frequency Analysis , Turbulent Flow , Spiral Flow , MEMS , Shear Stress Sensor .

1 INTRODUCTION

Our research group has been studying spiral flow. The spiral flow is a swirling flow with large free vortex region, high concentration to the axis and high stability [1]. From the characteristics, the spiral flow is useful for industrial applications such as an optical cord installation in a small diameter pipeline with bends[2] and high performance pneumatic transportation without particles touching pipe inner wall[3]. Accordingly, it is necessary to analyze near-wall shear stress of the spiral flow to improve the performance of the system, because the stability of materials optical cords and particles in solid-spiral flow two phase flow is affected by eddy structure which occurs near the wall.

Nowadays, micro-electro-mechanical-systems (MEMS) chip technology was developed to analyze the near wall shear stress by UCLA and Caltech [4]. This MEMS chip is a large-scale distributed control system with integrated micromachined transducers and microelectronic circuits for surface shear stress control. However, the distribution of stripe structure with MEMS chip is integral values that are composed of various kinds of frequency ingredients. It leads to make the stripe structure ambiguous.

Recently, wavelets transform has been popular for time-frequency analysis instead of Fourier transform in mechanical engineering fields. The merits of the wavelets analysis is to be able to analyze the frequency not to erase the time information. Wavelets transform [5] is roughly classified with two types, which are continuous wavelets transform and discrete wavelets transform. The continuous wavelets transform has been generally used for time frequency analysis in vibration wave. For example, self-similarity of the inner structure of the jet [6], the breakdown of a large eddy and the successive branching of a large eddy structure in a plane jet [7], decomposition of Reynolds stress in a jet [8], and the multiple acoustic modes and the shear layer instability [9] were investigated. However, most of the researchers on the time-frequency analysis carried out the continuous wavelets transform. On the other hand, the discrete wavelets transform has been mainly used for picture image processing. The analysis enables to decompose and to compose of picture image data quantitatively because of the orthonormal transform. Saito applied this idea to analyzing the electromagnetic wave[10].

The originality of this paper lies in applying the discrete wavelets transform to analyzing the wall shear stress obtained with the MEMS chip. In this study, the two dimensional shear stress in a turbulence boundary layer is decomposed from low frequency to high frequency levels with discrete wavelets transform to visualize the stripe structure in detail.

2 THEORY OF DISCRETE WAVELETS TRANSFORM

Basic concept of discrete wavelets transform is described using matrix expression instead of integral expression. One dimensional input data matrix **X** and an analyzing wavelets matrix **W** are used to simplify the expression. The wavelets transform matrix **S** is expressed by

$$\mathbf{S} = \mathbf{W} \cdot \mathbf{X} \tag{1}$$

The basic concept of the discrete wavelets transform is generalized by using fourth Daubechies function (N=4). The analyzing wavelets matrix **W** is acquired by a cascade algorithm on the basis of a function matrix **C**. The matrix **C** is shown in Eq. (2),

$$C=\begin{pmatrix} c_0 & c_1 & c_2 & c_3 & 0 & 0 & \cdots & 0 & 0 & 0 \\ c_3 & -c_2 & c_1 & -c_0 & 0 & 0 & \cdots & 0 & 0 & 0 \\ 0 & 0 & c_0 & c_1 & c_2 & c_3 & \cdots & 0 & 0 & 0 \\ 0 & 0 & c_3 & -c_2 & c_1 & -c_0 & \cdots & 0 & 0 & 0 \\ \cdots & \cdots & \cdots & \cdots & \cdots & \cdots & \cdots & \cdots & \cdots & \cdots \\ 0 & 0 & 0 & 0 & 0 & 0 & \cdots & c_0 & c_1 & c_2 & c_3 \\ 0 & 0 & 0 & 0 & 0 & 0 & \cdots & c_3 & -c_2 & c_1 & -c_0 \\ c_2 & c_3 & 0 & 0 & 0 & 0 & \cdots & 0 & 0 & c_0 & c_1 \\ c_1 & -c_0 & 0 & 0 & 0 & 0 & \cdots & 0 & 0 & c_3 & -c_2 \end{pmatrix} \begin{matrix} c_0=\frac{1+\sqrt{3}}{4\sqrt{2}} \\ c_1=\frac{3+\sqrt{3}}{4\sqrt{2}} \\ c_2=\frac{3-\sqrt{3}}{4\sqrt{2}} \\ c_3=\frac{1-\sqrt{3}}{4\sqrt{2}} \end{matrix} \tag{2}$$

$$c_3 - c_2 + c_1 - c_0 = 0 \tag{3}$$

$$0\,c_3 - 1\,c_2 + 2\,c_1 - 3\,c_0 = 0 \tag{4}$$

Where, $\mathbf{C}^T \cdot \mathbf{C} = \mathbf{I}$. The first line in Eq. (2) is called scaling coefficients and second line is called wavelets coefficients. Forth Daubechies function (N=4) has four coefficients in a line. The first line shows a transform to obtain a mean value with weights of c_0, c_1, c_2 and c_3 on the input data. The second line shows a transform to obtain a difference value with weights of c_0, c_1, c_2 and c_3 on the input data. The third line shows a transform to translate the first line by two steps. The fourth line is a transform to do the second line by two steps. Eqs. (3) and (4) show the transformed values are zero when the input data are constant or are simply increased. To explain easily the process to acquire the analyzing wavelets matrix **W** from **C**, the matrix **X** is assumed as one dimensional 16 elements,

$$\mathbf{X} = [x_1\ x_2\ x_3\ x_4\ x_5\ x_6\ x_7\ x_8\ x_9\ x_{10}\ x_{11}\ x_{12}\ x_{13}\ x_{14}\ x_{15}\ x_{16}]^T \tag{5}$$

From Eqs. (2) and (5), the transformed matrix **X'** is

$$\mathbf{X}' = \mathbf{C}_{16}\mathbf{X} = [s_1\ d_1\ s_2\ d_2\ s_3\ d_3\ s_4\ d_4\ s_5\ d_5\ s_6\ d_6\ s_7\ d_7\ s_8\ d_8]^T \tag{6}$$

Where, $\mathbf{C}_{16}$ is 16X16 matrix of **C**. The element s indicates the mean value and the element d indicates the difference value. The elements in the matrix **X'** are replaced by a matrix $\mathbf{P}_{16}$.

$$\mathbf{P}_{16}\mathbf{X}' = \mathbf{P}_{16}\,\mathbf{C}_{16}\mathbf{X} = [s_1\ s_2\ s_3\ s_4\ s_5\ s_6\ s_7\ s_8\ d_1\ d_2\ d_3\ d_4\ d_5\ d_6\ d_7\ d_8]^T \tag{7}$$

Where, $\mathbf{P}_{16}$ is defined as

$$\mathbf{P}_{16}=\begin{pmatrix} 1&0&0&0&0&0&0&0&0&0&0&0&0&0&0&0 \\ 0&0&1&0&0&0&0&0&0&0&0&0&0&0&0&0 \\ 0&0&0&0&1&0&0&0&0&0&0&0&0&0&0&0 \\ 0&0&0&0&0&0&1&0&0&0&0&0&0&0&0&0 \\ 0&0&0&0&0&0&0&0&1&0&0&0&0&0&0&0 \\ 0&0&0&0&0&0&0&0&0&0&1&0&0&0&0&0 \\ 0&0&0&0&0&0&0&0&0&0&0&0&1&0&0&0 \\ 0&0&0&0&0&0&0&0&0&0&0&0&0&0&1&0 \\ 0&1&0&0&0&0&0&0&0&0&0&0&0&0&0&0 \\ 0&0&0&1&0&0&0&0&0&0&0&0&0&0&0&0 \\ 0&0&0&0&0&1&0&0&0&0&0&0&0&0&0&0 \\ 0&0&0&0&0&0&0&1&0&0&0&0&0&0&0&0 \\ 0&0&0&0&0&0&0&0&0&1&0&0&0&0&0&0 \\ 0&0&0&0&0&0&0&0&0&0&0&1&0&0&0&0 \\ 0&0&0&0&0&0&0&0&0&0&0&0&0&1&0&0 \\ 0&0&0&0&0&0&0&0&0&0&0&0&0&0&0&1 \end{pmatrix} \tag{8}$$

Moreover, from Eq. (7), the transform is continuously carr 7 ied out by **C** and **P** without any operations to the difference values,

$$\mathbf{W}^{(2)}\mathbf{X} = [S_1\ S_2\ S_3\ S_4\ D_1\ D_2\ D_3\ D_4\ d_1\ d_2\ d_3\ d_4\ d_5\ d_6\ d_7\ d_8]^T \tag{9}$$

$$\mathbf{S} = \mathbf{W}^{(3)}\mathbf{X} = [S_1\ S_2\ D_1\ D_2\ D_1\ D_2\ D_3\ D_4\ d_1\ d_2\ d_3\ d_4\ d_5\ d_6\ d_7\ d_8]^T \tag{10}$$

Where,

$$\mathbf{W}^{(2)} = (\mathbf{P}_{16}'\mathbf{C}'_{16})(\mathbf{P}_{16}\mathbf{C}_{16}) \tag{11}$$

$$\mathbf{W}^{(3)} = (\mathbf{P}_{16}''\ \mathbf{C}_{16}'')(\mathbf{P}_{16}'\ \mathbf{C}_{16}')(\mathbf{P}_{16}\mathbf{C}_{16}) \tag{12}$$

$$\mathbf{P}_{16}'=\begin{bmatrix} \mathbf{P}_8 & 0 \\ 0 & \mathbf{I}_8 \end{bmatrix}\mathbf{C}_{16}'=\begin{bmatrix} \mathbf{C}_8 & 0 \\ 0 & \mathbf{I}_8 \end{bmatrix}\mathbf{P}_{16}''=\begin{bmatrix} \mathbf{P}_4 & 0 \\ 0 & \mathbf{I}_{12} \end{bmatrix}\mathbf{C}_{16}''=\begin{bmatrix} \mathbf{C}_4 & 0 \\ 0 & \mathbf{I}_{12} \end{bmatrix} \tag{13}$$

$\mathbf{W}^{(3)}$ is a analyzing wavelets matrix that is **W** in Eq. (1). The wavelets spectrum **S** in Eq. (1) is $\mathbf{W}^{(3)}\mathbf{X}$ in Eq. (10). In Eq. (9), S_1 indicates the mean value from s_1 to s_4 in Eq. (7). S_2 indicates the mean value from s_3 to s_6 that translate by two steps. D_1 indicates the difference value from s_1 to s_4. In Eq. (10), S_1 indicates the mean value from S_1 to S_4 in Eq. (9). D_1 indicates the difference value from S_1 to S_4 in Eq. (9). From Eq. (10), the input data are transformed to the mean values and the difference values with valuable resolution levels by the discrete wavelets transform. The input data are divided into a range from high frequency to low frequency.

From Eq. (10), the inverse wavelets transform is,

$$\mathbf{X} = [\mathbf{W}^{(3)}]^T\mathbf{S} \tag{14}$$

$$[\mathbf{W}^{(3)}]^T = [(\mathbf{P}_{16}''\mathbf{C}_{16}'')(\mathbf{P}_{16}'\mathbf{C}_{16}')(\mathbf{P}_{16}\mathbf{C}_{16})]^T = \mathbf{C}_{16}^T\mathbf{P}_{16}^T(\mathbf{C}_{16}')^T(\mathbf{P}_{16}')^T(\mathbf{C}_{16}'')^T(\mathbf{P}_{16}'')^T \tag{15}$$

From Eq. (14), the multiresolution is,

$$X = [W^{(3)}]^T S = [W^{(3)}]^T S_0 + [W^{(3)}]^T S_1 + [W^{(3)}]^T S_2 + [W^{(3)}]^T S_3 \quad (16)$$

Where,

$S_0 = [S_1\ S_2\ 0\ 0\ 0\ 0\ 0\ 0\ 0\ 0\ 0\ 0\ 0\ 0\ 0\ 0]^T$

$S_1 = [0\ 0\ D_1\ D_2\ 0\ 0\ 0\ 0\ 0\ 0\ 0\ 0\ 0\ 0\ 0\ 0]^T$

$S_2 = [0\ 0\ 0\ 0\ D_1\ D_2\ D_3\ D_4\ 0\ 0\ 0\ 0\ 0\ 0\ 0\ 0]^T$

$S_3 = [0\ 0\ 0\ 0\ 0\ 0\ 0\ 0\ d_1\ d_2\ d_3\ d_4\ d_5\ d_6\ d_7\ d_8]^T \quad (17)$

In the case of sixteen input data and fourth Daubechies, multiresolution indicates from Level 0 to Level 3.

3 EXPERIMENTS

3.1 Experimental setup

The experiment was carried out in a turbulent channel flow facility. The channel, constructed by 13 mm Plexiglas, was 610 mm x 25.4 mm in cross-section and 4880 mm long. An axial blower controlled by a DC power generates the air flow in the channel. The previous hot-wire measurement indicated that the channel flow, at a centerline velocity of 10 m/s, consists of a laminar entrance flow and a fully developed turbulent flow in the half downstream of the channel.

The shear-stress micro sensor [11] was plugged into the wall as the clearance between the top sensor plane and the top wall plane is zero. Fig. 1 shows top view of the micro shear stress sensor. Each micro sensor consists of polysilicon resistor wire of 150 μm long, 3 μm wide and 0.45 μm thick. The sensors have a vacuum cavity of thickness 2 μm in order to reduce the heat transfer and to increase the sensitivity of the sensor [12]. The sensors use the same circuits as a hot-wire anemometer and operate at an overheat ratio of 1.1. The shear-stress micro sensors has three sensors lines containing 25 sensors in one row, and the other two sensors lines contain 5 sensors in one row as shown in Fig. 2. Therefor, the shear-stress micro sensors consist of 85 sensors. The distance between the sensor arrays is 300 μm. The spanwise distribution of the turbulent surface shear stress had measured between length of 7.5 mm by 25 micro shear-stress sensors of one array. The experiment was carried out at Re's (=du_∞/v, where d=half width of the channel, u_∞ =centerline velocity) 8700and 17400.

3.2 Shear-stress distribution

Fig. 3 shows 2-D shear stess distributions measured by the 25 sensors covering an area 7.5 mm wide, 20 ms in time in two different Re numbers. Areas of high shear stress are marked by light-gray and low shear stress are shown dark-gray. The transverse scale of high shear-stress streaks varies with Re numbers. The streaks are narrow and packed more densely as Re number increases. These shear-stress distribution is decomposed with discrete wavelets transform at the next section.

4 ANALYSIS & DISCUSSION

The spectrums transformed with discrete wavelets transform are shown in Fig. 4. The spectrums are inversely transformed to each level with inverse wavelets transform and multiresolution analysis. Fig. 5 shows the multiresolution of the lower Re number, and Fig. 6 shows the multiresolution of the higher Re number (Level 6 is not shown). The values are normalized with the –0.2 minimum and 0.4 maximum to be shown at the ten level contour. From this multiresolution, the original shear-stress distribution in Fig. 3 can be clearly divided from low frequency level (Level 0) to high frequency level (Level 6) without erasing both of time and distance information. The white part is large value and dark part is small value. The summation from Level 0 to Level 6 recovers completely the original turbulence velocities in Fig. 5. In this figure the higher level symbolizes small vortex field, and lower level shows large vortex field.

In Fig. 5 and Fig. 6, as the frequency level is higher, the stripe structure become small gradually. In the case of Re=8700, the eddy stripe structure is clearly confirmed from Level 0 to Level 3. More than Level 4 components are regarded as noise domain. On the other hand, in the case of Re=17400, the eddy stripe structure exists from Level 0 to Level 4. Level 5 is noise domain. This new method visualizes the dominant level of eddy stripe structure. The stripe structure in high Re number appears even in high frequency field as composed with low Re number. Generally, the eddy in higher Re number can be divided into smaller eddy without disappearance by viscosity, because flow in high Re number has high Kolmogorov number. This phenomenon is confirmed by DNS (Direct Numerical Simulation). This new visualization method make it clear by a combination of MEMS technique and discrete wavelets transform.

5 CONCLUSIONS

The shear-stress on the wall in a turbulent boundary layer is decomposed by a combination of MEMS chip and discrete wavelets transform. As a result, shear stress can be clearly decomposed from low frequency to high frequency without erasing time and distance information. In the case of high Re number, a stripe structure appears in even high frequency domain.

ACKNOWLEDGMENTS

The authors wish to thank Dr. F. Jiang and Dr. Y.-C. Tai from the California Institute of Technology for the use of the micro shear stress image chip. We also appreciate the help from Mr. J. Hoffelner of University of Linz, Austria.

REFERENCES

1 Horii,K., (1990) Using Spiral Flow for Optical Cord Passing, *Mechanical Engineering - ASME*, Vol.112, No.8, pp68- 69

2 Horii,K. et al.,(1991) A Coanda Spiral Device Passing Optical Cords with Mechanical Connectors Attached through a Pipeline, *ASME FED-Vol.121, Gas-Solid Flows*, pp65-70.

3 Takei,M. et al., (1997) Transporting Particles without Touching Pipe Wall, *ASME FED*, FEDSM97-3629

4 Ho, C. M., Tung, S. and Tai, Y. C., 1996, "Interactive Control of Wall Structures by MEMS-Based Transducers," Advances in Turbulence , *Proceedings of the Sixth European Turbulence Conference*, pp.413, Lausanne, Switzerland, July.

5 Molet,F. et al., (1989) Wavelets Propagation and Sampling Theory, *Geophysics*, Vol.11

6 Everson,R. and Sirovich,L., (1990) Wavelets Analysis to the Turbulence Jet, Phys.Lett., Vol.145 No.6, pp314-322

7 Li,H. and Nozaki,T., (1995) Wavelets Analysis for the Plane Turbulence Jet (Analysis of large eddy structure), *JSME International Journal Fluids and Thermal Engineering*, Vol.38, No.4 pp525-531

8 Gordeyev,S.V. and Thomas,F.O., (1995) Measurement of Reynolds Stress Reversal in a Planar Jet by Means of a Wavelets Decomposition, *Turbulent Flows ASME*. FED-Vol.208. pp.49-54

9 Walker,S.H., Gordeyev,S.V. and Thomas,F.O., (1995)A Wavelets Transform Analysis Applied to Unsteady Jet Screech Resonance, *High speed jet flow ASME*. FED-Vol.214.pp103-108

10 Saito,Y., (1996)Wavelets Analysis for Computational Electromagnetics, (in Japanese), *Trans. IEE of Japan*, Vol. 116A, No10, pp833-839

11 Jiang, F., Tai, Y. C., Gupta, B., Goodman, R., Tung, S., Huang, J. B. and Ho, C. M., 1996, "A Surface-Micromachined Shear Stress Imager," *Proceedings of the 9th International IEEE Workshop on MEMS*, p.110, San Diego.

12 Huang, J. B., Tung, S., Ho, C. H., Liu, C., and Tai, Y. C., 1996, "Improved Micro Thermal Shear-Stress Sensor," IEEE transactions on Instrumentation and Measurement, Vol.45, No.2, pp.570.

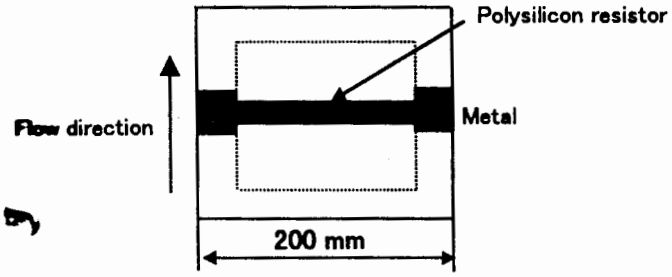

Fig.1 Schematic top view of the micro shear stress sensor

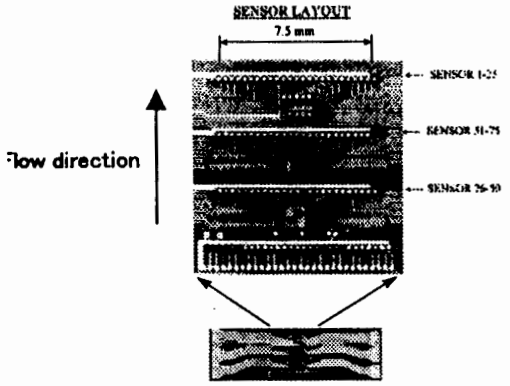

Fig.2 A surface shear stress imaging chip

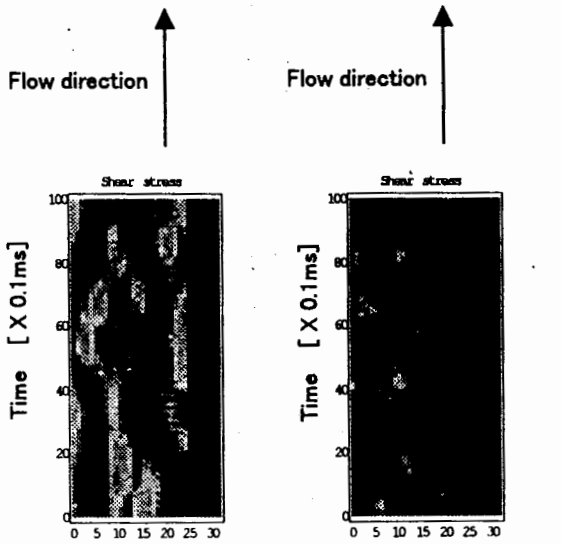

Fig.3 Instantaneous surface shear-stress measured by the imaging chip

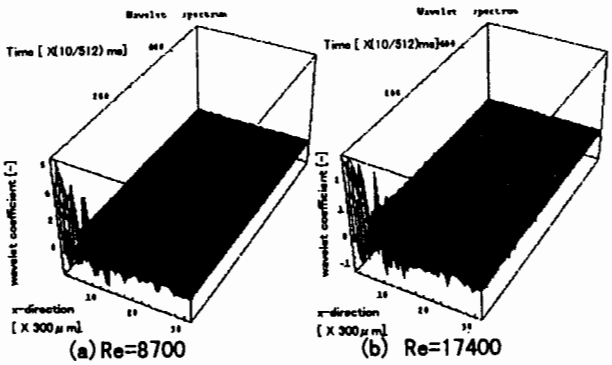

(a) Re=8700 (b) Re=17400

Fig. 4 Wavelet spectrum

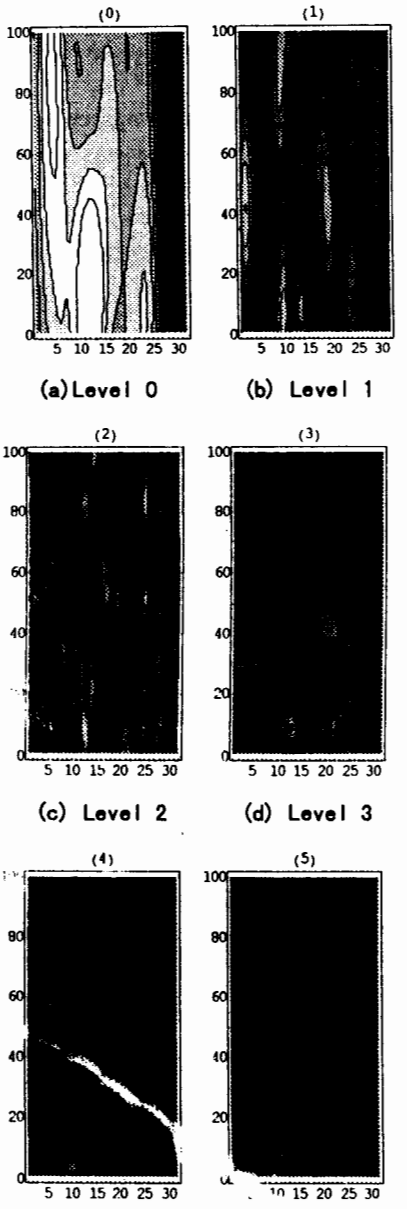

(a) Level 0 (b) Level 1
(c) Level 2 (d) Level 3
(e) Level 4 (f) Level 5

Fig.5 Multiresolution analysis in Re=8700

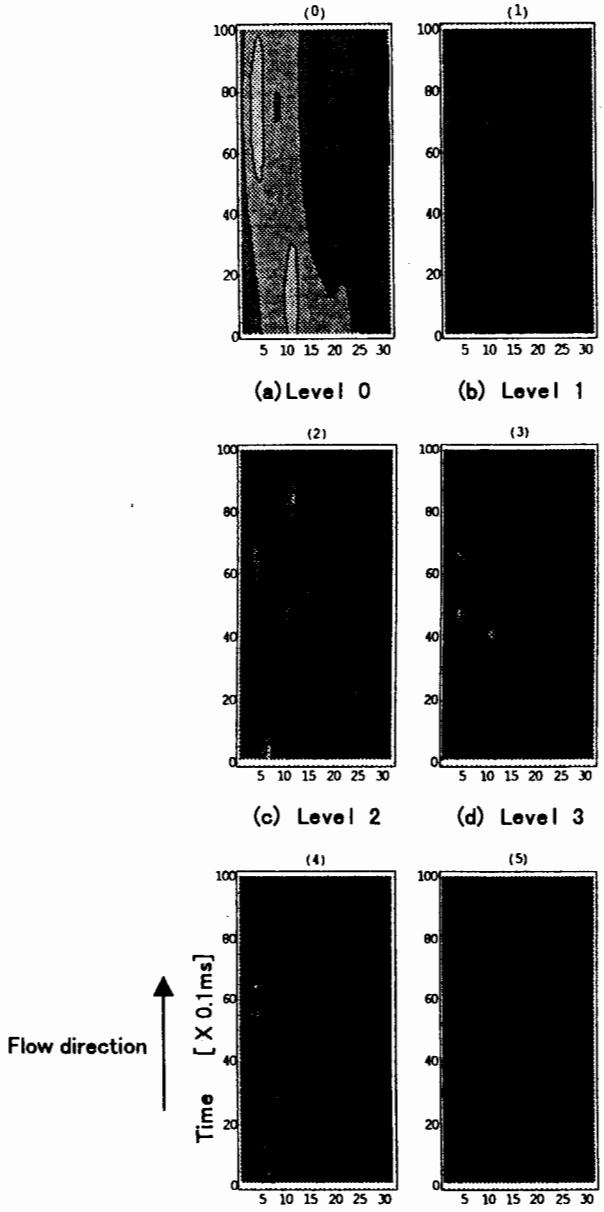

(a) Level 0 (b) Level 1
(c) Level 2 (d) Level 3
(e) Level 4 (f) Level 5

Fig.6 Multiresolution analysis in Re=17400